VOLUME 122, NUMBER 5
FEBRUARY 9, 2000

JOURNAL OF THE AMERICAN CHEMICAL SOCIETY

Zirconium-Mediated Metathesis of Imines: A Study of the Scope, Longevity, and Mechanism of a Complicated Catalytic System

Rebecca L. Zuckerman, Shane W. Krska, and Robert G. Bergman*

Contribution from the Department of Chemistry, University of California, Berkeley, California, 94720

Received July 23, 1999

Abstract: By kinetically stabilizing imidozirconocene complexes through the use of a sterically demanding ligand, or by generating a more thermodynamically stable resting state with addition of diphenylacetylene, we have developed transition metal-catalyzed imine metathesis reactions that are mechanistically analogous to olefin metathesis reactions catalyzed by metal carbene complexes. When 5 mol % of Cp*Cp(THF)Zr=N^{t}Bu is used as the catalyst precursor in the metathesis reaction between PhCH=NPh and *p*-TolCH=N-*p*-Tol, a 1:1:1:1 equilibrium mixture with the two mixed imines *p*-TolCH=NPh and PhCH=N-*p*-Tol is generated in C_6D_6 at 105 °C. The catalyst was still active after 20 days with an estimated 847 turnovers ($t_{1/2}$ 170 m; TON = 1.77 h^{-1}). When the azametallacyclobutene $Cp_2Zr(N(Tol)C(Ph)=C(Ph))$ is used as the catalyst precursor under similar reaction conditions, a total of 410 turnovers are obtained after 4 days ($t_{1/2}$ 170 m; TON = 4.3 h^{-1}). An extensive kinetic and equilibrium analysis of the metallacyclobutene-catalyzed metathesis of PhCH=N-*p*-Tol and *p*-F-C_6H_4CH=N-*p*-F-C_6H_4 was carried out by monitoring the concentrations of imines and observable metal-containing intermediates over time. Numerical integration methods were used to fit these data to a detailed mechanism involving coordinatively unsaturated (16-electron) imido complexes as critical intermediates. Examination of the scope of reaction between different organic imines revealed characteristic selectivity that appears to be unique to the zirconium-mediated system. Several zirconocene complexes that could generate the catalytically active "CpCp′Zr=NAr" (Cp′ = Cp or Cp*) species in situ were found to be effective agents in the metathetical exchange between different *N*-aryl imines. *N*-Alkyl aldimines were found to be completely unreactive toward metathesis with *N*-aryl aldimines, and metathesis reactions involving the two *N*-alkyl imines TolCH=NPr and PhCH=NMe gave slow or erratic results, depending on the catalyst used. Metathesis was observed between *N*-aryl ketimines and *N*-aryl aldimines, but for *N*-aryl ketimine substrates, the catalyst resting state consists of zirconocene enamido complexes, generated by the formal C−H activation of the α position of the ketimine substrates.

Introduction

Olefin metathesis has emerged as an important class of reactions in chemistry for the formation of new carbon−carbon double bonds.[1−4] These transformations have found widespread applications in organic synthesis[1,2] and polymer chemistry.[3,4] In contrast, analogous metal-catalyzed methods for selectively metathesizing double bonds to nitrogen (e.g., imines, diazenes) have been virtually unexplored until recently.[5−8]

* Author to whom correspondence should be addressed.

(1) Schuster, M.; Blechert, S. *Angew. Chem., Int. Ed. Engl.* **1997**, *36*, 2036.
(2) Grubbs, R. H.; Chang, S. *Tetrahedron* **1998**, *54*, 4413.
(3) Noels, A. F.; Demonceau, A. *J. Phys. Org. Chem.* **1998**, *11*, 602.
(4) Oskam, J. H.; Schrock, R. R. *J. Am. Chem. Soc.* **1993**, *115*, 11631.
(5) Cantrell, G. K.; Meyer, T. Y. *Organometallics* **1997**, *16*, 5381.
(6) Cantrell, G. K.; Meyer, T. Y. *J. Chem. Commun.* **1997**, 1551.
(7) Tóth, G.; Pintér, I.; Messmer, A. *Tetrahedron Lett.* **1974**, 735.

10.1021/ja992869r CCC: $19.00
Published on Web 01/25/2000

Scheme 1

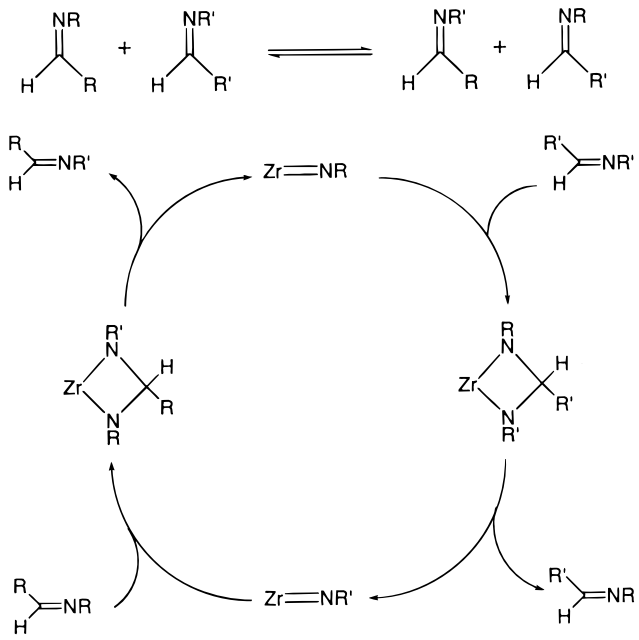

Scheme 2

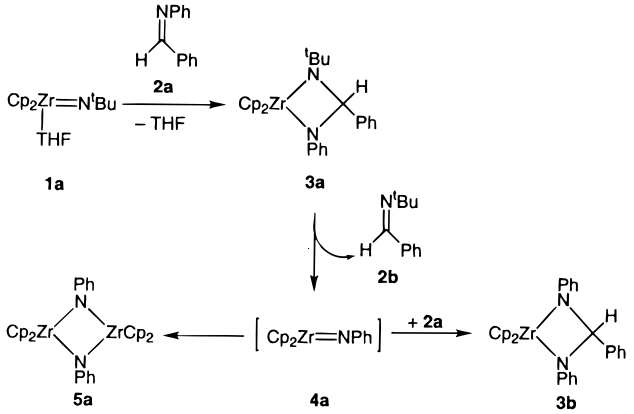

Scheme 1 illustrates a potential mechanism for imine metathesis catalyzed by zirconium imido complexes that is analogous to the pathway established for olefin metathesis catalyzed by metal alkylidene complexes. A Zr═NR species can react with an organic imine in an overall [2 + 2] cycloaddition reaction to generate a diazametallacyclobutane intermediate. Cycloreversion of this intermediate can occur in one of two directions, resulting either in a degenerate reaction or in the production of a new Zr═NR′ species along with a product imine. The newly formed imido species can react with a second reactant imine and undergo a similar pathway to regenerate the original Zr═NR species and release a second product imine.

Previous work in our laboratories demonstrated that stoichiometric imine metathesis reactions may be mediated by monomeric imidozirconocene complexes (Scheme 2).[9,10] Treatment of *N*-*tert*-butylimidozirconocene complex **1a** with 2 equiv of benzaldehyde *N*-phenylimine (**2a**) results in a stoichiometric exchange of imine N substituents accompanied by the formation of diazametallacycle **3b** and the imine PhCH═N^{t}Bu (**2b**). While stoichiometric imine metathesis is feasible with this system, attempts to carry out this reaction using catalytic amounts of **1a** were hindered by the irreversible formation of catalytically inactive dimeric species $[Cp_2Zr(NR)]_2$ (e.g., R = Ph, **5a**).

We report here our efforts to develop long-lived zirconium-based catalysts for the metathesis of imines. The activity and longevity of several catalysts have been examined. In addition, the scope of the metathesis reaction has been investigated with respect to the imine substrates. Finally, a series of kinetic experiments have been conducted in order to more fully understand the mechanism of the catalytic imine metathesis reaction. The results obtained from these studies are consistent with the mechanistic model shown in Scheme 1.[11]

Results

Catalytic Imine Metathesis of PhCH═NPh and *p*-TolCH═N-*p*-Tol. A study was carried out aimed at examining the activities and longevities of several different zirconium-based catalysts for the metathesis reaction between equimolar amounts of PhCH═NPh (**2a**) and *p*-TolCH═N-*p*-Tol (**2c**) to generate equilibrium mixtures (1:1:1:1) of **2a**, **2c**, PhCH═N-*p*-Tol (**2d**), and *p*-TolCH═NPh (**2e**) (Table 1; for a list of all imines utilized in the study, see Table 2). When 5 mol % of $Cp_2(THF)Zr$═N(2,6-$Me_2C_6H_3$) (**1b**) was used as the catalyst in C_6D_6 at 105 °C, the $t_{1/2}$ of the reaction was measured to be 8 min. Based upon the appearance of the ^{1}H NMR spectrum of the reaction mixture, the resting state for the catalyst under these conditions was determined to be the statistical mixture of diazametallacyclobutane complexes that form from the reaction of free Cp_2Zr═NPh and Cp_2Zr═N-*p*-Tol with the reactant and product imines. This conclusion is supported by the intense purple color of the metathesis reaction mixture, which is the same color as that observed for solutions of isolated diazametallacyclobutane complexes (vide infra).

Upon continued heating, the metathesis reaction mixture developed a green color, with accompanying new signals in the ^{1}H NMR spectrum. After 24 h at 105 °C, the formation of a green precipitate was noted. At this point the solution was no longer catalytically active, as demonstrated by the observed lack of reaction upon addition of further amounts of the reactant imines. The green precipitate was assumed to be a mixture of dimeric bridging imido complexes that have partial solubility in C_6D_6. To confirm the identity of one of the zirconium-containing species in solution, the dimer $[Cp_2ZrN$-*p*-Tol$]_2$ (**5b**) was independently synthesized by heating $Cp_2Zr(N(H)(-p$-Tol$))$-(Me) in THF at 95 °C for several days (eq 1). Comparison of

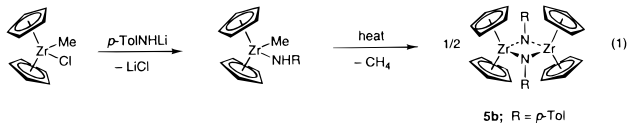

(1)

5b; R = *p*-Tol

the ^{1}H NMR spectrum of **5b** with that of the metathesis reaction mixture confirmed the presence of the dimeric species **5b** in the mixture. Additionally, the green precipitate was isolated and MS analysis confirmed the identity of **5b**. To determine whether this dimer was capable of cycloreversion to generate the catalytically active zirconocene imido complex under the reaction conditions, 5 mol % of **5b** was heated to 105 °C in the

(8) (a) McInnes, J. M.; Mountford, P. *Chem. Commun.* **1998**, 1669. (b) McInnes, J. M.; Blake, A. J.; Mountford, P. *J. Chem. Soc. Dalton Trans.* **1998**, 3623.

(9) Meyer, K. E.; Walsh, P. J.; Bergman, R. G. *J. Am. Chem. Soc.* **1995**, *117*, 974.

(10) Meyer, K. E.; Walsh, P. J.; Bergman, R. G. *J. Am. Chem. Soc.* **1994**, *116*, 2669.

(11) Portions of this work have been communicated previously. Krska, S. W.; Zuckerman, R. L.; Bergman, R. G. *J. Am. Chem. Soc.* **1998**, *120*, 11828.

Table 1. Half-Lives ($t_{1/2}$ Values) for Metathesis Reactions

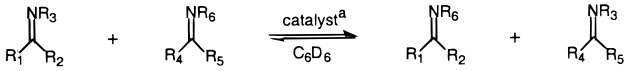

temp (°C)	starting imines	R_1	R_2	R_3	starting imines	R_4	R_5	R_6	$t_{1/2}$ (min) **1a**	**1b**	**6a**	**10a**
105	**2a**	Ph	H	Ph	**2c**	p-Tol	H	*p*-Tol	14	8	70	780
135	**2i**	Ph	H	Me	**2h**	p-Tol	H	*n*-Pr	10	NR	NR	*b*
135	**2l**	Ph	Me	Ph	**2c**	p-Tol	H	*p*-Tol		12		
135	**2m**	*t*-Bu	H	*p*-Tol	**2a**	Ph	H	Ph	NR	NR	257	NR
150	**2i**	Ph	H	Me	**2f**	p-Tol	H	*p*-$MeOC_6H_4$	NR	NR	NR	NR

[a] Catalyst = **1a**, **1b**, **6a**, or **10a**. [b] Incomplete reaction. NR = no reaction.

Table 2. Imines Utilized in the Study

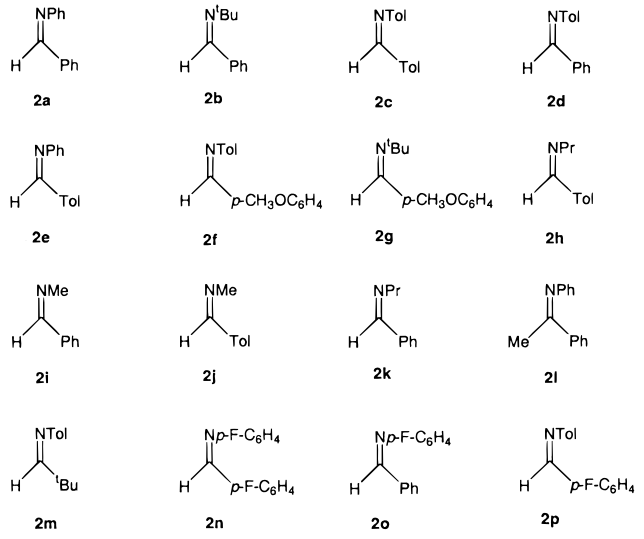

presence **2a** and **2c**. There was no metathesis observable by ^{1}H NMR after 51 h.

To increase the longevity of the imidozirconocene catalysts, some method was sought to inhibit or, if possible, eliminate the formation of the catalytically inactive dimeric species. Diphenylacetylene has been shown to bind strongly to imidozirconocene complexes, forming azametallacyclobutene adducts.[12−15] Because the dimerization reaction is necessarily second-order in the free imidozirconocene species, the addition of such a strongly binding ligand might be expected to slow the dimerization process dramatically by sequestering the active species in a more stable resting state. Azametallacyclobutene complexes **6a**,**b** were therefore synthesized as outlined in eq 2

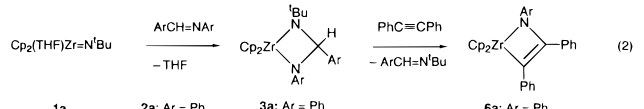

and tested as catalysts for the metathesis reaction. Their synthesis involved treatment of diazametallacycles **3a**,**c** (generated in situ by the reaction of **1a** with 1 equiv of the corresponding imine, **2a**,**c**), with 1 equiv of diphenylacetylene at 45 °C for ca. 7 h, which afforded the desired azametallacyclobutene products **6a**,**b** in good yields after recrystallization.

When complex **6a** was used as the catalyst under the standard metathesis reaction conditions, metathesis occurred, but the rate was slowed by a factor of 9 relative to the reaction with **1b** as catalyst (Table 1). The reaction mixture was a deep green color, typical of azametallacyclobutene complexes **6**. Analysis of the reaction mixture by ^{1}H NMR spectroscopy under working metathesis conditions revealed metallacyclobutene complexes **6a** and **6b** as the predominant (>90%) Zr-containing species, although minor amounts of diazametallacyclobutane complexes could also be detected. No dimeric species were observed, even after heating for 4 days at 105 °C.[16] In contrast to experiments with **1a**, the catalyst was still active at this time (total turnovers ca. 410), which was demonstrated by adding more imine starting materials to the system and observing the reinitiation of metathesis. Similar results could be obtained by generating the metallacyclobutene catalyst in situ using an equimolar mixture of **1a** and diphenylacetylene.

The equilibrium constant for the azametallacyclobutene/diazametallacyclobutane interchange under the metathesis reaction conditions was determined by heating complexes **6a**,**b** in the presence of excess amounts of the corresponding imine (**2a**,**d**), and measuring the relative concentrations of the species involved by ^{1}H NMR spectroscopy (eq 3). For the interconversion of **6a** and **3b**, $K_{eq} = 1.8 \times 10^{-3}$ at 75 °C; for **6b** and **3d**, $K_{eq} = 1.2 \times 10^{-3}$ at 105 °C.[17] To confirm the presence of diazametallacycles **3b**,**d** in the equilibrium mixtures, authentic samples were synthesized independently from zirconocene imido **1a** and 2 equiv of the corresponding imine (eq 4), and their

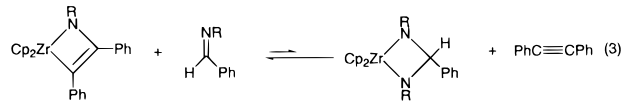

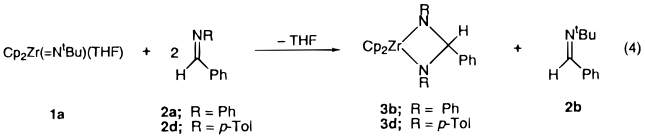

(12) Walsh, P. J.; Hollander, F. J.; Bergman, R. G. *Organometallics* **1993**, *12*, 3705.

(13) Baranger, A. M.; Walsh, P. J.; Bergman, R. G. *J. Am. Chem. Soc.* **1993**, *115*, 2753.

(14) Walsh, P. J.; Baranger, A. M.; Bergman, R. G. *J. Am. Chem. Soc.* **1992**, *114*, 1708.

(15) Lee, S. Y.; Bergman, R. G. *Tetrahedron* **1995**, *51*, 4255.

(16) A slow side reaction between diphenylacetylene and the reactant and product imines was catalyzed by **6b**. This resulted in the complete consumption of diphenylacetylene over a period of 4 days, leaving diazametallacycles **3** as the predominant Zr-containing species.

(17) The previously reported K_{eq} value of 7.4 for the **6a**/**3a** interconversion at 70 °C is incorrect because of the misinterpretation of spectroscopic data. The equilibrium value was remeasured at 75 °C at three different concentrations of **3a**, and the spectral data were compared with those for authentic samples of **6a** and **3a**.

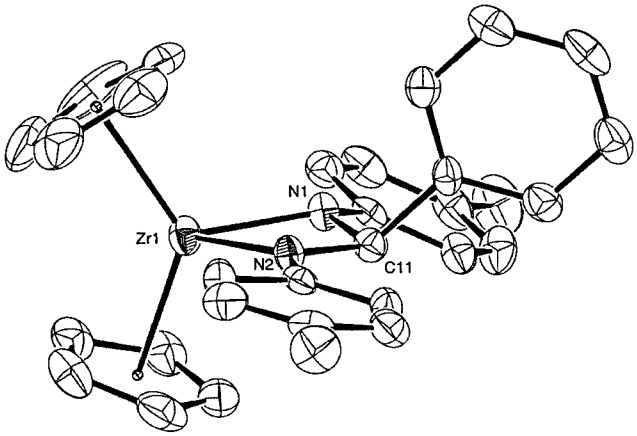

Figure 1. ORTEP diagram of diazametallacycle **3d**. The thermal ellipsoids are scaled to represent the 50% probability surface.

Table 3. Selected Bond Lengths (Å) and Bond Angles (deg) for Compounds **3d**, **10a**, **10b**, and **13b**

	bond lengths			
compd	Zr1−N1	Zr1−N2	Zr1−O1	N2−C26
3d	2.093(4)	2.091(4)		
10a	1.846(2)		2.285(2)	
10b	1.881(3)		2.281(2)	
13b	2.070(3)	2.239(2)		1.426(4)

	bond angles			
compd	N1−Zr1−N2	N1−Zr1−O1	Zr1−N1−C16	Zr1−N2−C26
3d	66.1(1)			
10a		92.75(9)	169.5(2)	
10b		93.52(10)	168.4(2)	
13b	100.8(1)			121.9(2)

NMR spectroscopic data were compared to those obtained in the equilibrium experiments.[9,10]

Crystals of purple diazametallacycle **3d** suitable for X-ray diffraction were obtained by cooling a hexane solution at −35 °C for 1 day. The ORTEP diagram for **3d** is shown in Figure 1. The Zr−N bond distances are equal (2.09 Å) (Table 3), and are typical for zirconocene amido complexes.[12,18,19] The diazametallacyclobutane ring is slightly puckered, with C11 deviating from the mean plane calculated through Zr1, N1, and N2 by 0.2 Å in the direction opposite to the phenyl ring.

Synthesis and Catalytic Activity of (η^5-C_5H_5)(η^5-C_5Me_5)-(THF)Zr(=NR) Complexes. A second strategy for increasing the lifetime of the imidozirconocene catalyst involves using increased steric bulk around the metal center to inhibit the dimerization reaction. This may be accomplished by replacing one of the Cp ligands of the imido complex with a Cp* (pentamethylcyclopentadienyl) ligand. The synthetic pathway to prepare CpCp*(THF)Zr(=N^{t}Bu), **10a**, is outlined in Scheme 3. Treatment of the previously reported[20] dimethyl complex **7** with 1 equiv of $Me_3NH^+Cl^-$ afforded methyl chloride complex **8** in high yield and 95% purity (the balance of the material was $CpCp^*ZrMe_2$ and $CpCp^*ZrCl_2$). The reaction of complex **8** with LiNH^{t}Bu gave the methyl amide complex **9**, which upon thermolysis in THF at 95 °C for 3 days generated imido complex **10a**. Recrystallization from toluene layered with hexanes gave **10a** as yellow blocks in 55% yield. One of these crystals was

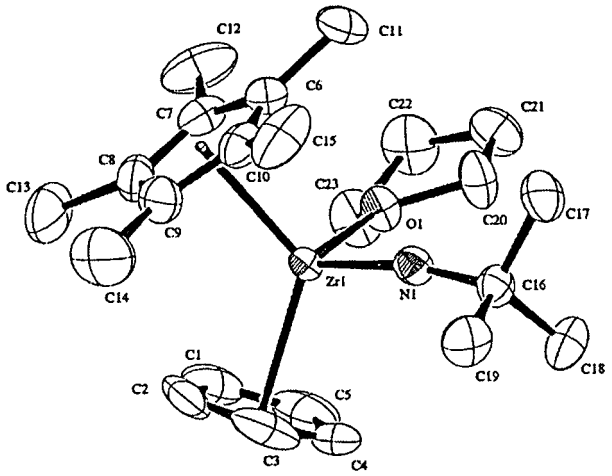

Figure 2. ORTEP digram of CpCp*(THF)Zr=N^{t}Bu (**10a**). The thermal ellipsoids are scaled to represent the 50% probability surface.

Scheme 3

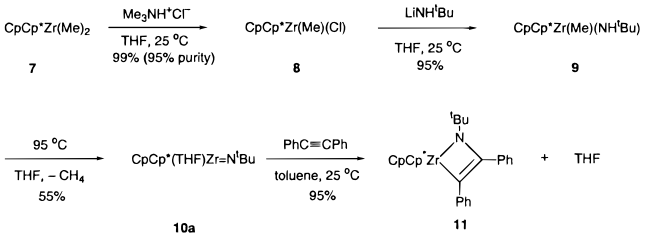

analyzed by X-ray diffraction, and the ORTEP diagram is shown in Figure 2. The Zr−N bond distance in **10a** was found to be 1.846(2) Å, 0.02 Å longer than the corresponding distance (1.826(4) Å) in **1a**.[12] In addition, the imido linkage in **10a** was slightly more bent (∠Zr−N−C = 169.5(2)°) than that of **1a** (174.4(3)°) (Table 3). Both of these structural features imply a slightly lower Zr−N bond order in **10a** than **1a**. This may be a consequence of the more highly electron-donating Cp* ligand in **10a** which reduces the extent of π-donation from the imido lone pair to the empty metal-centered b_2 antibonding orbital.[21]

Imido complex **10a** reacts with stoichiometric amounts of organic imines to give diazametallacyclobutane complexes **12** (eq 5). Upon mixing **10a** and an imine such as *p*-$CH_3OC_6H_4$-

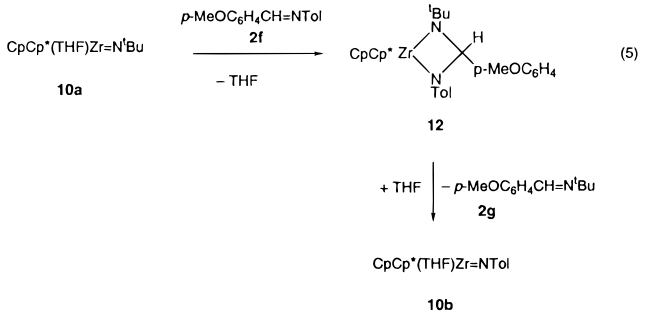

(5)

CH=N-*p*-Tol (**2f**) in C_6D_6, there was an immediate color change from yellow to rose. Analysis of the reaction mixture by ^{1}H NMR spectroscopy revealed what is tentatively identified as the two diastereomers of the expected metallacycle **12**, resulting from an overall [2 + 2] cycloaddition reaction between **10a** and **2f**. Over a matter of hours at 25 °C, the solution began to assume a brick-red color. ^{1}H NMR spectroscopy showed the appearance of a new product with a concurrent disappearance of the metallacycles. From the spectroscopic data, it appeared

(18) Cardin, D. J.; Lappert, M. F.; Raston, C. L.*Chemistry of Organo-Zirconium and -Hafnium Compounds*; Ellis Horwood: New York, 1986.
(19) Arney, D. J.; Bruck, M. A.; Huber, S. R.; Wigley, D. E. *Inorg. Chem.* **1992**, *31*, 3749.
(20) Wolczanski, P. T.; Bercaw, J. E. *Organometallics* **1982**, *1*, 793.
(21) Green, J. C. *Chem. Soc. Rev.* **1998**, *27*, 263.

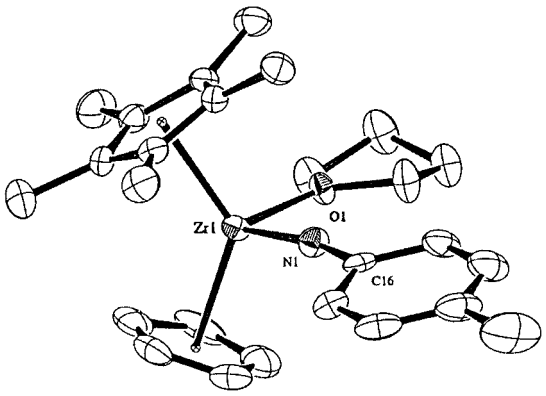

Figure 3. ORTEP diagram of CpCp*(THF)Zr═NTol (**10b**). The thermal ellipsoids are scaled to represent the 50% probability surface.

that cycloreversion of the metallacycle was occurring with the extrusion of imine **2g** and the formation of N-*p*-Tol imido complex **10b**. This is in marked contrast to the behavior of the bis(cyclopentadienyl) system, where only the dimeric species of the general formula $[Cp_2Zr(NAr)]_2$ are isolated when there are no ortho substituents on the aryl ring to sterically prevent the dimerization reaction.

Repeating the reaction between **10a** and **2f** on a preparative scale resulted in the isolation of imido complex **10b** in 67% yield. X-ray quality crystals were obtained by slow diffusion of hexanes into a toluene solution of **10b** at −35 °C. An ORTEP diagram of **10b** is shown in Figure 3. The imido Zr−N bond length is 1.881(3) Å, 0.035 Å longer than that of **10a**. Consistent with the longer Zr−N bond in **10b** was its Zr−N−C angle of 168.4(2)°, which deviated further from linearity than that of **10a** (Table 3). That imido complex **10b**, which has a smaller N substituent than **10a**, should exhibit a longer Zr−N bond length and a more bent Zr−N−C angle is consistent with the notion that electronic factors as opposed to steric factors are responsible for these subtle structural variations in the zirconium imido subunit.[22]

When complex **10a** was used as the catalyst under the standard metathesis reaction conditions (using imines **2a** and **2c**), a slow but constant rate was observed (Table 1). Analysis of the purple reaction mixture by ^{1}H NMR spectroscopy indicated the presence of a statistical mixture of diazametallacyclobutane complexes similar to **12**. The catalyst was still active after 20 days at 105 °C (giving a total of ca. 850 TO), and there was no spectroscopic evidence for the formation of dimeric species.

Control Experiments. Since both acids[7] and bases[8] have been shown to catalyze imine metathesis, several control experiments were carried out to establish that the metathesis observed in the present system was not due to the presence of trace amounts of acidic or basic impurities. In the first control experiment, equimolar amounts of imines **2a** and **2c** were subjected to the usual reaction conditions in the absence of catalyst; no metathesis was observed, even after 51 h of heating. This result ruled out the possibility that impurities in the solvent or on the surface of the glassware were responsible for the observed metathesis.

A second set of control experiments involved the use of Cp_2ZrMe_2 as a trap for adventitious water or acidic impurities.[23] As a test of this method, an equimolar mixture of **2a** and **2c** containing 5 mol % of *p*-toluic acid was heated in C_6D_6 to 105 °C in the presence and absence of 10 mol % of Cp_2ZrMe_2.

(22) Williams, D. S.; Korolev, A. V. *Inorg. Chem.* **1998**, *37*, 3809.
(23) Proulx, G.; Bergman, R. G. *Organometallics* **1996**, *15*, 684.

Scheme 4

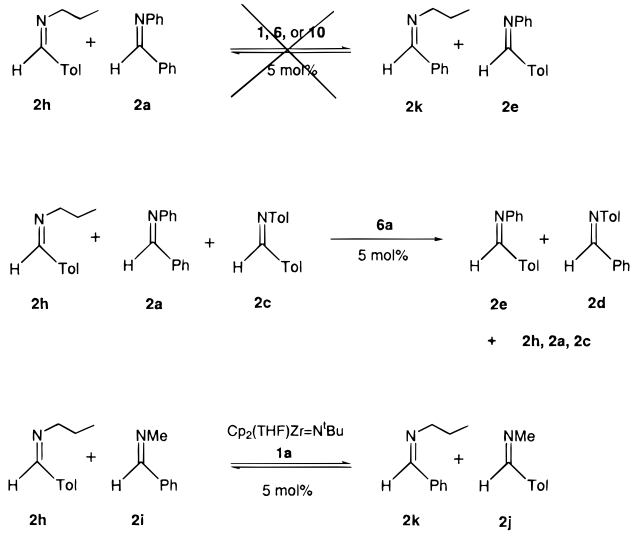

Complete metathesis was observed in the latter case after 30 min of heating, but it was completely suppressed in the former case, even after extended heating (19 h) with ca. 50% of the added Cp_2ZrMe_2 still remaining by ^{1}H NMR. Performing the imidozirconocene-catalyzed metathesis reactions of **2a** and **2b** in the presence of Cp_2ZrMe_2 gave different results, depending on the catalyst. Complexes **1b** and **6a** exhibited shorter lifetimes in the presence of Cp_2ZrMe_2 (giving a total of three and nine turnovers, respectively). However, both of these catalysts were independently shown to react with Cp_2ZrMe_2 to give several unidentified products. On the other hand, complex **10a** was shown to react much more slowly with Cp_2ZrMe_2 and demonstrated undiminished catalytic activity in its presence.

Scope of the Metathesis Reaction. Reactions of *N*-Alkyl Aldimines. Among the various classes of imines tested as substrates for the metathesis reaction were *N*-alkyl aldimines (Table 1). These exhibited very different reactivity than their *N*-aryl counterparts. For example, *N*-alkyl aldimines were found to be completely unreactive toward metathesis with *N*-aryl aldimines using imidozirconocene-based catalysts. Treating an equimolar mixture of *p*-TolCH═NPr (**2h**) and PhCH═NPh (**2a**) with the various catalysts shown in Table 1 and Scheme 4 resulted in no observable metathesis, even at elevated temperatures (up to 150 °C). In addition, a green precipitate formed during heating when **1a**, **1b**, or **6a** were used as catalysts, indicative of dimer formation. When an equimolar mixture of two *N*-aryl aldimines (**2a** and **2c**) and an *N*-alkyl aldimine (**2h**) was heated (105 °C) in the presence of catalyst (**6a**), metathesis occurred only between the two *N*-aryl aldimines, leaving the *N*-alkyl aldimine unreacted (Scheme 4). Thus, the imidozirconocene catalysts were found to be active in the presence of *N*-alkyl imines, but unable to catalyze the metathesis of *N*-alkyl with *N*-aryl imines.

Metathesis reactions involving two *N*-alkyl imines, TolCH═NPr (**2h**) and PhCH═NMe (**2i**) gave different results depending on the catalyst used. No metathesis was observed under any conditions using **1b** or **6a** as catalysts. When **10a** was employed as catalyst, metathesis occurred at 135 °C, but the reaction ceased at less than 50% conversion. In contrast to the poor activities found for **1b**, **6a**, and **10a**, complex **1a** effectively catalyzed the metathesis of *N*-alkyl imines **2h** and **2i** in C_6D_6 at 135 °C (5 mol % of **1a**) to give an equilibrium mixture of

Scheme 5

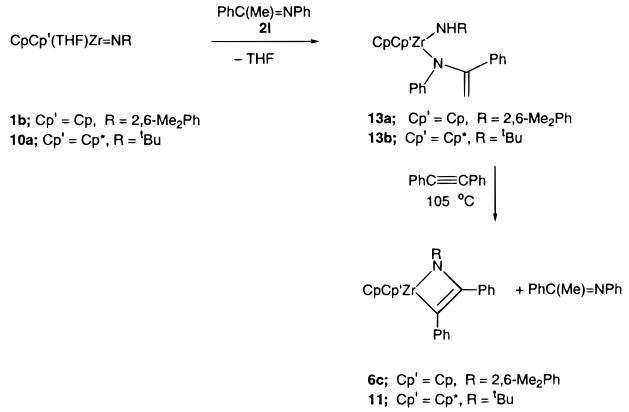

2h, **2i**, TolCH═NMe (**2j**), and PhCH═NPr (**2k**). The measured $t_{1/2}$ for the reaction was <10 min.[24]

Reactions of the Ketimine Ph(Me)C═NPh. Several of the imidozirconocene catalysts in Table 1 were found to effectively catalyze the metathesis reaction between *N*-aryl ketimine Ph(Me)C═NPh (**2l**) and *N*-aryl aldimine **2c**. However, two unusual features of these reactions were noted. First, the metathesis reaction mixtures did not display the purple color typical of diazametallacyclobutane complexes **3**, and instead were orange in color. In addition, the reactions were very slow at 105 °C and required heating to 135 °C to proceed at reasonable rates.

To understand better the nature of the reactivity of ketimine **2l** with imidozirconocene complexes, stoichiometric reactions of complexes **1b** and **10a** with **2l** were carried out (Scheme 5). These reactions did not afford diazametallacyclobutane complexes, but instead gave enamido complexes **13a**,**b** in quantitative yield (by ^{1}H NMR spectroscopy). Complexes **13a**,**b** were isolated as crystalline solids in high yields and identified by their characteristic ^{1}H NMR spectra. These contained two olefinic resonances in the δ 5.6 to 4.5 ppm range along with a broad NH resonance at 6.4 (for complex **13a**) and 4.6 ppm (for complex **13b**). Complex **13b** was further characterized by X-ray crystallography (as a hexane solvate). An ORTEP diagram is shown in Figure 4. All bond lengths and angles are consistent with the structure drawn in Scheme 5. One notable feature of the structure is the somewhat large disparity between the Zr1−N1 and Zr1−N2 bond lengths (2.070(3) and 2.239(2) Å, respectively) (Table 3), which can be attributed to delocalization of the N2 lone pair into the π-system of the enamido ligand (sum of angles about N2 = 359.6°).

When either **13a** or **13b** was heated in C_6D_6 at 105 °C in the presence of diphenylacetylene, the corresponding azametallacyclobutene complex was formed in quantitative yield along with 1 equiv of **2l**, according to ^{1}H NMR spectroscopy (Scheme 5). The identity of the product metallacyclobutenes was confirmed by comparison with the spectral data of independently synthesized samples (e.g., see Scheme 3). This provides evidence that complexes **13a**,**b** reversibly generate the corresponding free imidozirconocene species at elevated temperatures, and these are subsequently trapped by diphenylacetylene to form azametallacyclbutene complexes **6c** and **11**. In accord with this observation, complexes **13a**,**b** were also found to be competent catalysts for the metathesis of **2l** with **2c** (5 mol % catalyst, 135 °C).

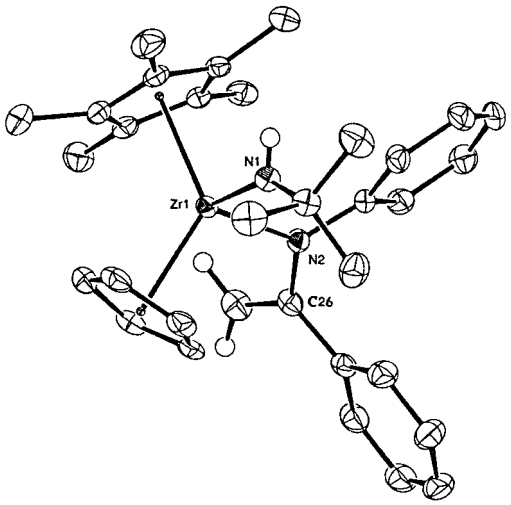

Figure 4. ORTEP diagram of **13b**. The thermal ellipsoids are scaled to represent the 50% probability surface.

Table 4. Initial Concentrations of Reactants and Catalyst Used in Kinetic Runs

run	[**2d**]$_0$ (M)	[**2n**]$_0$ (M)	[**6b**]$_0$ (M)	[Ph−C≡C−Ph]$_0$ (M)
1	0.302	0.101	0.0381	0.0409
2	0.134	0.297	0.0254	0.0304
3	0.268	0.165	0.0316	0.0360
4	0.399	0.237	0.0252	0.0295
5	0.200	0.464	0.0271	0.0310
6	0.302	0.333	0.0297	0.0322
7	0.0973	0.281	0.0173	0.0209
8	0.151	0.101	0.0183	0.0212

Reactions of the *C*-Alkyl Aldimine ^{t}BuCH═N-*p*-Tol. The final class of imine substrate examined in the metathesis reaction bore an alkyl substituent (^{t}Bu) on the imine carbon atom in place of the usual aryl group. Metathesis between this sterically hindered substrate (^{t}BuCH═N-*p*-Tol; **2m**) and **2a** occurred only when complex **6a** (5 mol %) was used as the catalyst (Table 1). The reaction required elevated temperatures (135 °C) and proceeded much more slowly ($t_{1/2}$ = 257 min) than the corresponding metathesis reaction involving only *C*-aryl aldimines, consistent with the high steric demand of the C-^{t}Bu substituent of **2m**.

Kinetic Studies. To gain further insight into the mechanism of the catalytic imine metathesis reaction, a series of kinetic experiments were undertaken. Azametallacyclobutene **6b** was employed as catalyst for these studies due to its stability under the reaction conditions.[25] Reactions were run in sealed NMR tubes and monitored by ^{1}H NMR spectroscopy. The imines PhCH═N-*p*-Tol (**2d**) and *p*-F-C_6H_4CH═N-*p*-F-C_6H_4 (**2n**) were chosen as starting materials because the CH resonances for these compounds and their metathesis products, PhCH═N-*p*-F-C_6H_4 (**2o**) and *p*-F-C_6H_4CH═N-*p*-Tol (**2p**), are resolved well enough to guarantee accurate quantification of concentration by NMR integration. To maintain a constant concentration of diphenylacetylene throughout the reaction, 1 equiv of alkyne was added relative to the catalyst.[26] Reactions were run at different catalyst concentrations using several different ratios of the two reactant

(24) The stoichiometric reaction between **1a** and **2i** was carried out to gain further understanding of the metathesis reaction between **2i** and **2h** in the presence of 5 mol % **1a**. Unlike the *N*-aryl cases, a diazametallacycle was spectroscopically observed as a possible intermediate in the generation of a new dinuclear zirconmium species that was crystallographically characterized as $(Cp_2Zr)_2$(*m*-NH^{t}Bu)(*m*-N═CH_2). The details of this study have been published independently (*J. Organomet. Chem.*, **1999**, *591*, 2).

(25) Complex **10a** was not chosen as the catalyst precursor for the kinetic measurements because its imine adducts analogous to **3** exist as pairs of diastereomers. It was thought that this would further complicate the already complex system.

(26) The K_{eq} measurements in eq 3 predict that, at equilibrium, less than 10% of **6b** should be converted to diazametallacyclobutanes **3**.

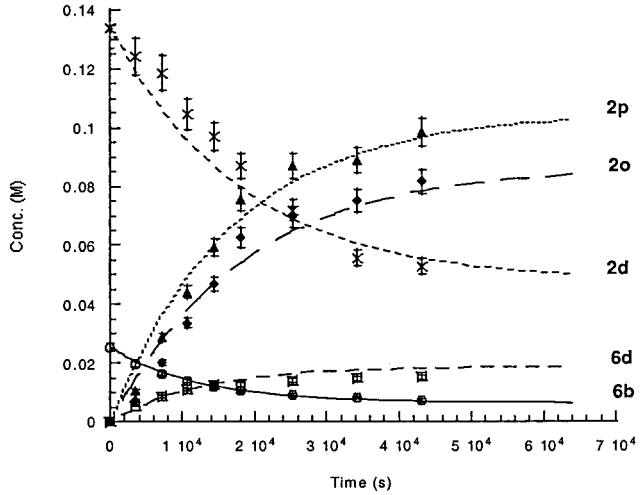

Figure 5. Experimentally determined (points) and simulated (lines) concentration vs time profiles for the reactant and product imines and the two azametallacyclobutene complexes **6b** and **6d** for a representative kinetic run. Error bars assume 10% uncertainty in NMR integration.

imines (Table 4). The concentrations of imines, the two azametallacyclobutenes, and diphenylacetylene were monitored with time.

Based upon the mechanistic evidence presented in the preceding sections, the metathesis reaction involving catalyst **6b** is proposed to occur according to the mechanism presented in Scheme 6. The complexity of this kinetic model necessitated the use of kinetic simulation software[27] to derive rate constants from the experimental kinetic data. For this purpose, the 20 microscopic rate constants shown in Scheme 6 were reduced to six distinguishable parameters, k_R, k_T, k'_{RT}, k'_{RF}, k'_{TT}, and k'_{TF}, based on reasonable assumptions about the relative rates of these elementary steps. The rates of reversion (k_R) of metallacyclobutene complexes **6b** and **6d** were assumed to be equal, as were the rates of trapping (k_T) of the transient imido species **4b** and **4c** with diphenylacetylene. The rates of cycloreversion of diazametallacycles **3d**,**f**,**g**,**i** to release N-*p*-Tol imines were set equal to the parameter k'_{RT}. Likewise, the rates of cycloreversion of complexes **3e**,**g**−**i** to release N-*p*-F-C_6H_4 imines were set equal to k'_{RF}. The rates of trapping of the transient imido complexes **4b** and **4c** with N-*p*-Tol (k'_{TT}) and N-*p*-F-C_6H_4 (k'_{TF}) imines constituted the final two parameters.

By application of a nonlinear least-squares fitting routine,[27] the kinetic model described above was simultaneously fit to the experimental concentration vs time data for all eight kinetic runs. The rate constants derived from this optimization are given in Scheme 6. The tolerances associated with these values were estimated by varying each parameter independently and determining the point at which the goodness-of-fit of the simulation was significantly reduced. For most of the kinetic runs, the agreement between the experimental data and the simulated curves was found to be satisfactory; a sample plot is shown in Figure 5.[28]

The dependence of the goodness-of-fit of the model on the six parameters was examined by varying them independently. The overall fit of the model was most sensitive to the parameter k_R, changing significantly even with small variations (<10%)

Scheme 6

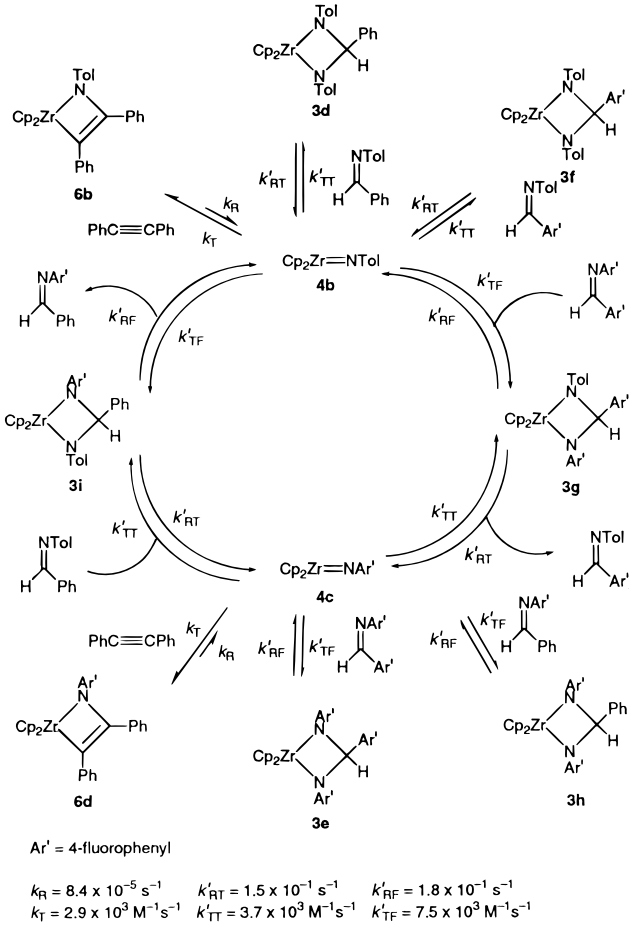

in the rate constant. The fit of the model showed a smaller, although not negligible, dependence on the parameters k'_{RT} and k'_{RF}.[29] In contrast, the model was insensitive to the absolute magnitude of the trapping rate constants k_T, k'_{TT}, k'_{TF}, although the ratio $k_T/(k'_{TT} + k'_{TF})$ determined the relative rates of imine metathesis and **6b**/**6d** equilibration. Finally, the ratio $k_R(k'_{TT} + k'_{TF})/k_T(k'_{RT} + k'_{RF})$, which is essentially equivalent to the equilibrium constants described in eq 3, strongly affected the fit of the model, because it controlled the absolute concentrations of metallacyclobutenes **6b** and **6d** in the simulated reaction mixture. Because of these different responses of the fit to changes in the rate constants, we estimate that the tolerances in k_R and k_T as approximately ± 10%, k_{TT}' as ±15% and k_{TF}' as ±35%.

Discussion

Development of Robust Imine Metathesis Catalysts. Previous studies indicated that monomeric imidozirconocene complexes were capable of mediating stoichiometric imine metathesis reactions (Scheme 2).[9,10] However, to develop a useful *catalytic* version of these reactions, the inherent tendency of the imidozirconocene species to dimerize irreversibly had to be overcome.

Two approaches were explored to eliminate this deleterious pathway. The first involved generating a more thermodynamically stable resting state for the catalyst by adding the ligand diphenylacetylene. This strategy took advantage of the fact that

(27) The FORTRAN programs GEAR and GIT (v. 2.1) were used for all kinetic simulations. (a) McKinney, R. J.; Weigert, F. J. Project SERAPHIM. Program number 1b-1407.8. (b) Weigert, F. J. *Comput. Chem.* **1987**, *11*, 273. (c) Stabler, R. N.; Chesick, J. *Int. J. Chem. Kinet.* **1978**, *10*, 461.

(28) Further examples of concentration vs time plots for the experimental and kinetic data are available as Supporting Information.

(29) Changing the parameters k_R (ca. 10^{-3} s^{-1}) and k'_{RT} (10^{-2} s^{-1}) also resulted in a reasonable fit for the experimental versus simulated data. However, these rate constants are not consistent with the measured K_{eq} value for the interconversion of **6b** and **3d**.

the unwanted dimerization reaction is necessarily second-order in the active imido species, whereas the imine metathesis reaction is presumably first-order in this species. By decreasing the effective concentration of the active imidozirconocene species through its complexation with diphenylacetylene, we expected the dimerization reaction to be slowed, much more so than the catalytic metathesis reaction. This proved to be the case. Although the metathesis reaction using catalyst **6a** was slowed by a factor of 9 relative to that using catalyst **1a** (Table 1), the dimerization reaction was no longer observed, increasing the catalyst lifetime. The dynamic equilibrium between the new metallacyclobutene catalyst resting state and the diazametallacyclobutane complexes responsible for imine metathesis was confirmed by ^{1}H NMR spectroscopic studies (eq 3). Based on the measured equilibrium constants, the difference in stability for the two species was on the order of 5 kcal/mol.

The second approach to increasing the catalyst lifetime involved disfavoring dimer formation through increased steric bulk around the zirconium metal center. Imidozirconocene complex **10a** bearing a sterically bulky Cp* ligand (Scheme 3) was found to be an effective catalyst for the metathesis of *N*-aryl aldimines. The mechanism of imine metathesis involving this species appears to be the same as that of catalysts **1a** and **1b**, involving diazametallacyclobutane intermediates. These complexes imparted a distinctive purple color to metathesis reaction mixtures involving **10a**, and were directly observable by ^{1}H NMR spectroscopy. Catalyst **10a** was extremely long-lived, retaining its catalytic activity even after 20 days at 105 °C. There was no spectroscopic evidence for the formation of any dimeric species.

Scope of Metathesis Reaction. The scope of the metathesis reaction involving the various imidozirconocene catalysts was examined with respect to several classes of imines (Table 1). Although all of the catalysts examined were effective for the metathesis of *N*-aryl aldimines, none of these catalysts were able to effect the metathesis of *N*-alkyl imines with *N*-aryl imines. Only one of the complexes examined (**1a**) was able to effectively catalyze the metathesis of two *N*-alkyl imines, and this catalyst, when mixed with two *N*-aryl imines and one *N*-alkyl imine, selectively metathesized only the *N*-aryl imines, leaving the *N*-alkyl imine unreacted (Scheme 4). The reasons for this selectivity are not entirely clear but may be due to a much stronger binding affinity of *N*-aryl imines for the active imido species, coupled with a preference for *N*-alkyl, *N*-aryl diazametallacyclobutanes to preferentially cyclorevert to generate *N*-alkyl imines and *N*-aryl imidozirconocene species. It should be mentioned that other reported imine metathesis catalysts (e.g., (DME)Cl_2Mo(=NR)$_2$,[5,6] and various acids[7]) do not show this selectivity.

Imine metathesis reactions involving *N*-aryl ketimines exhibited different catalyst resting states than the reactions involving only *N*-aryl aldimines. These new resting states were identified as enamido complexes **13a**,**b**, generated by the stoichiometric reactions between imidozirconocene complexes **1b** and **10a** and ketimine **2l** (Scheme 5). Complexes **13a**,**b** arise from formal C−H activation of the α position of ketimine **2l**. The reversibility of this reaction was demonstrated by heating **13a**,**b** in the presence of diphenylacetylene to give azametallacyclobutene complexes **6c** and **11** in quantitative yields (Scheme 5). Isolated complexes **13a**,**b** were also found to be effective catalysts for imine metathesis. Thus, it appears that ketimines exhibit a dual mode of reactivity with imidozirconocene species: C−H activation to give stable enamido complexes and cycloaddition to give diazametallacyclobutane complexes. The latter are not observed but lead to imine metathesis (Scheme 7).

Scheme 7

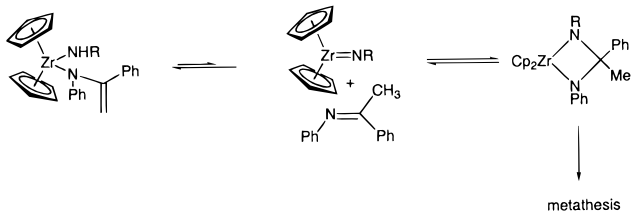

The metathesis reaction of the *C*-alkyl aldimine **2m** demonstrated the effect of placing a sterically demanding ^{t}Bu substituent on the C position of the imine. This substrate reacted only with the less-hindered bis(cyclopentadienyl) catalyst **6a**, and then only at a very sluggish rate at elevated temperatures (see Table 1).

Kinetic Studies. The most notable aspect of the previously reported stoichiometric imine metathesis reaction (shown in Scheme 2) was that it operated by a well-defined, kinetically characterizable mechanism that was directly analogous to olefin metathesis (Scheme 1).[2] The extension of this chemistry to a catalytic imine metathesis reaction would constitute the first example of catalytic C=X (X = heteroatom) metathesis demonstrated to proceed in an analogous manner to C=C metathesis catalyzed by metal alkylidene complexes. Preliminary spectroscopic studies indicated that catalytic imine metathesis did indeed occur by a mechanism similar to that of the stoichiometric reaction. For example, ^{1}H NMR analysis of the *N*-aryl aldimine metathesis reactions catalyzed by complex **6a** suggested that azametallacyclobutene complexes **6** were in equilibrium with diazametallacyclobutane complexes **3** (eq 3); these latter complexes were presumably responsible for the observed imine metathesis (cf. Scheme 2).[9,10] To provide more evidence for this mechanism, kinetic studies were undertaken of the metathesis reaction between PhCH=N-*p*-Tol (**2d**) and *p*-F-C_6H_4CH=N-*p*-F-C_6H_4 (**2n**) catalyzed by complex **6b**.

The kinetic runs listed in Table 4 were conducted using widely varying concentrations of imines and catalyst. The concentrations of five separate species (**2d**, **2o**, **2p**, **6b**, and **6d**) in the reaction mixtures were monitored over time. These data were simultaneously fit to the model shown in Scheme 6 using six parameters (k_R, k_T, k'_{RT}, k'_{RF}, k'_{TT}, and k'_{TF}; number of data points/parameter = 53). The result was a satisfactory agreement between the model's predictions and the experimentally determined concentration vs time profiles (e.g., Figure 5).[28]

The magnitudes of the rate constants derived from the model are summarized in the form of a free-energy diagram in Figure 6. Moving from left to right in this diagram, the slowest step in the catalytic cycle (k_R) was found to be the cycloreversion of azametallacyclobutene complexes **6b** and **6d** (whose ΔG_{rel} at 105 °C in Figure 6 was arbitrarily set to 0 kcal/mol), giving the free imido species **4b**,**c**. The free energy of activation for this process was calculated from k_R to be 29.3 kcal/mol, in good qualitative agreement with the corrected[17] value obtained from the previous stoichiometric studies (29.9 kcal/mol at 70 °C).[9,10] Since this is the rate-determining step of the catalytic cycle, its associated parameter (k_R) had the strongest effect on the goodness-of-fit of the simulation.

The rates of trapping of the transient imido species **4b**,**c** with alkyne (k_T) and imines (k'_{TT}, k'_{TF}) were of the same order of magnitude, consistent with prior results determined for the stoichiometric system.

The rates of cycloreversion of diazametallacyclobutane complexes **3d**−**i** (k'_{RT}, k'_{RF}) depended only weakly on the nature

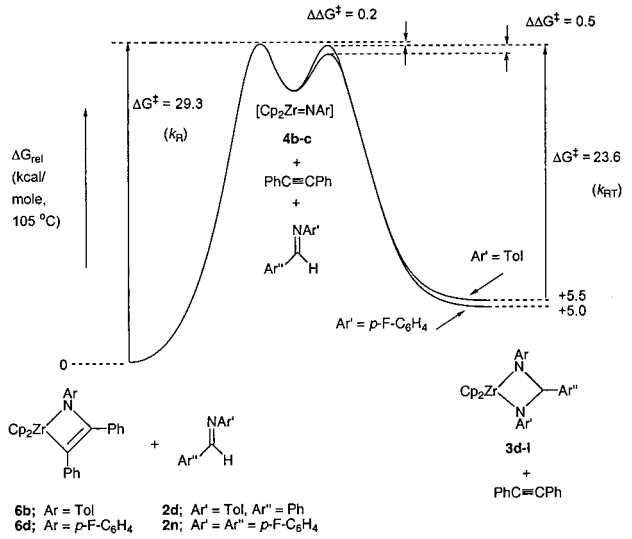

Figure 6. Free-energy diagram for catalytic imine metathesis (for explanation of compound labels, see Scheme 6).

of the *N*-aryl substituent of the imine. The free energies of activation for the extrusion of N-*p*-Tol and N-*p*-F-C_6H_4 imines from the corresponding diazametallacyclobutanes **3** were calculated (from k'_{RT} and k'_{RF}) to be 23.6 and 24.1 kcal/mol, respectively. These values compare favorably to the value previously determined for the cycloreversion of metallacycle **3b** (24.9 kcal/mol at 70 °C).[9,10] That the rates of trapping and cycloreversion involving imines were found to be only weakly dependent on the electronic nature of the imine substituents provided justification for the simplification of the kinetic model in Scheme 6 to include only 6 distinguishable parameters instead of the 20 possible rate constants. As a final note, it should be emphasized that the difference in stability between the metallacyclobutene complexes **6b**,**d** and the diazametallacyclobutane complexes **3d**−**i** shown in Figure 6 (on the order of 5 kcal/mol) was in close agreement with the experimentally determined value of 5.0 kcal/mol for the **6b**/**3d** interconversion shown in eq 3.[17,30]

Conclusions

Long-lived catalysts for the metathesis of *N*-aryl aldimines and ketimines have been developed based on imidozirconocene complexes. The mechanism of action of these catalysts involves formal [2 + 2] cycloaddition reactions between the imine substrates and the active imidozirconocene catalysts, giving diazametallacyclobutane intermediates. A series of kinetic and spectroscopic experiments has convincingly demonstrated that the mechanism of the catalytic metathesis is directly analogous to that of the well-known and widely used olefin metathesis reaction.

The resting state of the catalysts varies with the nature of the imine substrates and the presence of additives. In the absence of additives, the metathesis of *N*-aryl aldimines involves diazametallacyclobutane complexes as the catalyst resting state. For the bis(cyclopentadienyl) system, these complexes are not of sufficient stability relative to the free imido species to prevent the rapid formation of the catalytically inert dimeric bridging imido complexes. For the pentamethylcyclopentadienyl analogues, however, the dimerization reaction is sterically inhibited, and the catalysts are extremely long-lived. For the bis(cyclopentadienyl) system, in the presence of the additive diphenylacetylene, the catalyst resting state shifts to the more stable azametallacyclobutene complexes, and the lifetime of the catalyst is greatly increased. For *N*-aryl ketimine substrates, the catalyst resting state consists of zirconocene enamido complexes, generated by the formal C−H activation of the α position of the ketimine substrates.

(30) The parameters chosen initially for the experimental data fitting were based on rate constants experimentally determined from previous kinetic studies of the stoichiometric reactions. These parameters were then adjusted to obtain the best fit for the eight experimental runs. Final optimization of the model was accomplished by application of a nonlinear least-squares fitting routine. Simulations were allowed to converge, then restarted at the convergence point. This process was repeated until no further variations were seen in the rate constants. Rate constants obtained after convergence were still in agreement with independently measured equilibrium and rate constants.

Experimental Section

General Procedures. Unless otherwise noted, reactions and manipulations were performed using standard drybox or Schlenk techniques. Glassware was dried overnight at 150 °C before use. Unless otherwise noted, ^{1}H NMR spectra were recorded at 500 MHz and chemical shifts (δ) are reported in parts per million (ppm) relative to residual protiated solvent: C_6D_6 (7.15 ppm), THF-d_8 (3.58 ppm). Unless otherwise noted, $^{13}C\{^1H\}$ NMR were recorded at 100 MHz and are reported in ppm relative to the carbon resonance of the deuterated solvent: C_6D_6 (128.0 ppm), THF-d_8 (67.57 ppm). Elemental analyses were performed at the University of California—Berkeley Microanalytical facility.

Materials. Unless otherwise noted, reagents were purchased from commercial suppliers and used without further purification. Solvents were distilled from the appropriate drying agents under N_2 or passed through a column of activated alumina and sparged with N_2 prior to use. Complexes **1a**,[12] **1b**,[12] **6a**,[9,10] **6c**,[13] and **7**[20] were synthesized according to literature procedures. All lithium amides, LiNHR, were prepared by deprotonating the parent amine with 1.0 equiv of *n*-BuLi.

Imines were synthesized according to the standard procedure[31] of condensing the parent aldehyde or ketone and amine in C_6H_6 over dried 4 Å molecular sieves and either recrystallized (solids) or dried over 4 Å molecular sieves (liquids) prior to use. Product imines generated from the metathesis reactions between parent imines were independently synthesized and their ^{1}H NMR data were compared with literature values,[31] or their identity was confirmed by GC-MS analysis.[31,32] Characterization data were not found in the literature for *p*-F-C_6H_4-CH═N-*p*-F-C_6H_4 (**2n**). This imine was prepared by the standard procedure stated above, and characterization data are listed below.

Diazametallacycles **3a** and **3b** were synthesized according to literature procedures.[9,10] Diazametallacycles **3c** and **12** were generated in situ as intermediates in the synthesis of **6b** and **10b**, respectively, and were tentatively identified by their ^{1}H NMR data. Diazametallacycle **3d** was characterized by X-ray crystallographic analysis, and spectroscopic characterization data for this compound are listed below. Metallacycles **3e**−**i** were tentatively assigned by their ^{1}H NMR data and are transient intermediates outlined in Scheme 6 in the metathesis reaction between PhCH═N-*p*-Tol (**2d**) and *p*-F-C_6H_4CH═N-*p*-F-C_6H_4 (**2n**).

***p*-F-C_6H_4CH═N-*p*-F-C_6H_4 (2n).** White crystals. ^{1}H NMR (C_6D_6): δ 7.84 (s, 1H, aldimine C*H*), 7.56 (m, 2H, aryl), 6.89 (m, 2H, aryl), 6.81 (m, 2H, aryl), 6.72 (m, 2H, aryl) ppm. ^{13}C NMR (C_6D_6): δ 164.91 (d, J_{C-F} = 251 Hz, aryl), 161.64 (d, J_{C-F} = 245 Hz, aryl), 158.08 (*C*H═N), 148.31 (d, J_{C-F} = 4 Hz, aryl), 132.99 (d, J_{C-F} = 2.5 Hz, aryl), 122.66 (d, J_{C-F} = 7 Hz, aryl), 116.05 (d, J_{C-F} =14 Hz, aryl), 115.87 (d, J_{C-F} = 14 Hz, aryl) ppm. IR (NaCl disk): 756 (w), 844 (vs), 1090 (m), 1152 (w), 1185 (w), 1218 (m), 1245 (s), 1054 (s), 1590 (m), 1603 (s), 1628 (s), 2855 (w). Anal. Calcd $C_{13}H_9F_2N$: C, 71.88; H, 4.18; N, 6.45. Found: C, 71.89; H, 4.11; N, 6.36.

Cp_2Zr(N(Tol)CH(Ph)N(Tol)) (3d). A glass reaction vessel equipped with a Teflon stopcock was charged with Cp_2(THF)Zr═N^{t}Bu (**1a**) (120 mg, 0.33 mmol) and 5 mL of C_6H_6. The solution was stirred and PhCH═NTol (**2d**) (129 mg, 0.66 mmol, 2 equiv) was added dropwise,

(31) Bolognese, A.; Mazzoni, O.; Giordano, F. *Tetrahedron* **1991**, *47*, 7417.

(32) Nongkunsan, P.; Ramsden, C. *Tetrahedron* **1997**, *53*, 3805.

with a noted color change from yellow to purple upon the addition of PhCH═NTol. The mixture was heated at 45 °C for 7 h. Removing the solvent at reduced pressure left a purple solid which was dissolved in Et_2O (2 mL) and stored at −35 °C for 1 day to give purple crystals (140 mg, 81% yield). ^{1}H NMR (C_6D_6): δ 7.69 (d, J_{H-H} = 9.0 Hz, 2H, aryl), 7.01 (m, 4H, aryl), 6.90 (d, J_{H-H} = 8.5 Hz, 4H), 6.24 (s, 5H, C_5H_5), 5.91 (s, 5H, C_5H_5), 5.47 (s, 1H, C*H*), 2.25 (s, 6H, CH_3) ppm. ^{13}C NMR (C_6D_6): δ 50.91, 142.72, 129.86, 128.66, 128.54, 127.15, 125.87, 116.11(aryl), 114.91, 114.68 (C_5H_5), 63.27 (CH), 20.72 (CH_3) ppm. Repeated attempts to obtain elemental analysis on this complex were not successful. It has been characterized by X-ray diffraction.

$Cp_2Zr[N(^tBu)CH(p\text{-}F\text{-}C_6H_4)N(p\text{-}F\text{-}C_6H_4)]$ (3k). A glass reaction vessel equipped with a Teflon stopcock was charged with Cp_2-(THF)Zr═N^{t}Bu (**1a**) (188 mg, 0.515 mmol) and 7 mL C_6H_6. The yellow solution was stirred and *p*-F-C_6H_4CH═N-*p*-F-C_6H_4 **(2n)** (112 mg, 0.515 mmol, 1 equiv) was added dropwise with an immediate color change to maroon. A heterogeneous mixture formed during stirring at 25 °C for 2 h, and the resulting solid was isolated and triturated with hexanes (2 × 1 mL). The last traces of solvent were removed at reduced pressure to afford 186 mg (71% yield) of a rose powder. ^{1}H NMR (THF-d_8): δ 7.51 (m, 2H, aryl), 6.95 (m, 2H, aryl), 6.67 (m, 2H, aryl), 6.60 (s, 5H, C_5H_5), 6.30 (s, 5H, C_5H_5), 4.94 (s, 1H, C*H*), 0.96 (s, 9H, ^{t}Bu) ppm. ^{13}C NMR (THF-d_8): δ 163.0 (d, J_{C-F} = 242 Hz, aryl), 156.2 (d, J_{C-F} = 230 Hz, aryl), 150.4 (aryl), 141.5 (d, J_{C-F} = 15.1 Hz, aryl), 129.2, 116.5, 115.4, 115.3 (aryl), 115.1 (C_5H_5),114.3 (C_5H_5), 64.55 *C*H), 56.60 (^{t}Bu *C*), 31.98 (^{t}Bu *C*H$_3$) ppm. Anal. Calcd $C_{27}H_{28}F_2N_2Zr$: C, 63.62; H, 5.54; N, 5.50. Found: C, 63.34; H, 5.73; N, 5.39.

$[Cp_2Zr(\mu\text{-}p\text{-}Tol)]_2$ (5b). Method A. Cp_2Zr(Me)(Cl) (678 mg, 2.43 mmol) and *p*-TolC_6H_4NHLi (267 mg, 2.43 mmol, 1 equiv) were dissolved in THF (5 mL). The solution was stirred overnight and solvent was removed at reduced pressure to leave a yellow solid. The resulting solid was redissolved in C_6H_6 and filtered through Celite to remove residual LiCl. The filtrate was concentrated in vacuo to afford 700 mg (88% yield) of the corresponding complex Cp_2Zr(Me)(NH-*p*-Tol), which was then dissolved in THF (10 mL). The solution was heated for 2 days at 95 °C in a constant temperature silicon oil bath. During this time, kelly-green crystals precipitated out of the solution. The crystals were isolated (569 mg, 85% yield).

Method B. Cp_2(THF)Zr═N^{t}Bu (**1a**) (258 mg, 0.709 mmol) and TolCH═NTol (**2c**) (148 mg, 0.709 mmol, 1 equiv) were dissolved in C_6D_6 (7 mL), and the resulting purple solution was heated at 105 °C in a constant temperature silicon oil bath for 3 h. The resulting heterogeneous green mixture was filtered to afford 120 mg (52% yield) of **5b**. The filtrate was evaporated at reduced pressure to leave a green solid which was then triturated with Et_2O (2 mL) and filtered to obtain an additional 75 mg of **5b** (84% combined yield). ^{1}H NMR (CD_2Cl_2): δ 6.90 (d, J_{H-H} = 7.5 Hz, 4H, aryl), 6.44 (s, 20H, C_5H_5), 5.67 (d, J_{H-H} = 8.0 Hz, 4H, aryl), 2.70 (s, 6H, CH_3) ppm. ^{13}C NMR (CD_2Cl_2): δ 155.5, 128.8, 126.5, 120.6 (aryl), 133.0 (C_5H_5), 20.7 (CH_3) ppm. Anal. Calcd $C_{34}H_{34}N_2Zr_2$: C, 62.53; H, 5.25; N, 4.29. Found: C, 62.24; H, 4.96; N, 4.34.

$Cp_2Zr(N(Tol)C(Ph)═C(Ph))$ (6b). Diphenylacetylene (148 mg, 0.832 mmol, 1 equiv) and Cp_2(THF)Zr═N^{t}Bu (**1a**) (303 mg, 0.832 mmol) were dissolved in 5 mL of C_6H_6. A green color developed immediately. The solution was stirred for 5 min at 25 °C, and PhCH═NPh (149 mg, 0.832 mmol, 1 equiv) was added. The mixture was heated at 105 °C for 3 h and solvent was removed at reduced pressure to obtain a green solid, which was dissolved in toluene (2 mL) and stored at −35 °C for 1 day. The solvent was removed in vacuo to afford 337 mg of forest-green crystals (83% yield). ^{1}H NMR (C_6D_6): δ 7.27 (d, J_{H-H} = 7.5 Hz, 2H, aryl), 7.21 (t, J_{H-H} = 7.5 Hz, 2H, aryl), 7.05 (t, J_{C-H} = 8 Hz, 4H, aryl), 6.97 (d, J_{H-H} = 8 Hz, 3H, aryl), 6.96 (d, J_{H-H} = 7 Hz, 2H, aryl), 5.84 (s, 10H, C_5H_5), 2.14 (s, 3H, CH_3) ppm. ^{13}C NMR (C_6D_6): δ 151.1, 148.2, 132.7, 128.4, 128.3, 127.8, 127.2, 126.9, 123.5, 122.5, 121.1 (aryl and alkenyl), 112.0 (C_5H_5), 20.7 (CH_3) ppm. HRMS (EI): *m*/*z* calcd for $C_{31}H_{27}NZr$ 504.1207 (M^+), found 504.1200.

$Cp_2Zr(N(p\text{-}F\text{-}C_6H_4)C(Ph)═C(Ph))$ (6d). Diphenylacetylene (57 mg, 0.318 mmol, 2 equiv) and $Cp_2Zr[N(^tBu)CH(p\text{-}F\text{-}C_6H_4)N(p\text{-}F\text{-}C_6H_4)]$ (**3k**) (80.8 mg, 0.159 mmol) were dissolved in 5 mL of C_6H_6. The solution was heated at 45 °C for 10 h, resulting in a color change from purple to green. The solvent was removed under reduced pressure to obtain a green solid, which was dissolved in Et_2O (2 mL) and stored at −35 °C for 1 day. Forest-green crystals (58 mg, 78% yield) were obtained. ^{1}H NMR (C_6D_6): δ 7.20 (m, 4H, aryl), 7.0 (m, 3H, aryl), 6.92 (m, 3H, aryl), 6.72 (t, J_{H-H} = 8 Hz, 2H, aryl), 6.10 (m, 2H, aryl), 5.78 (s, 10H, C_5H_5) ppm. ^{13}C NMR (C_6D_6): δ 182.3 (aryl), 148.8 (d, J_{C-F} = 235 Hz, aryl), 149.8, 147.9, 132.18, 129.7, 128.6, 128.4, 127.6, 127.0, 123.7, 121.9 (aryl), 121.2 (d, J_{C-F} = 6 Hz, aryl), 115.2 (d, J_{C-F} = 22 Hz, aryl), 112.3 (C_5H_5) ppm. HRMS (EI): *m*/*z* calcd for $C_{30}H_{24}$-FNZr 507.0940 (M^+), found 507.0942. Anal. Calcd $C_{30}H_{24}FNZr$: C, 70.83; H, 4.75; N, 2.75. Found: C, 70.48; H, 4.67; N, 2.62.

Cp*CpZr(Me)Cl (8). A solution of **7** (3.27 g, 10.2 mmol) in ca. 10 mL of THF was added to a slurry of Me_3NHCl in 10 mL of THF. The reaction mixture was stirred at room temperature for 4 days, and then the volatile materials were removed at reduced pressure. The remaining white solid was extracted with ca. 15 mL of toluene, and the resulting solution was filtered and evaporated to leave a white crystalline solid (3.43 g, 99%). Analysis of this material by ^{1}H NMR indicated that it was 95% pure (the balance being Cp*CpZrMe$_2$ and Cp*CpZrCl$_2$). Analytically pure material could be obtained by repeated crystallization from toluene/hexanes. ^{1}H NMR (C_6D_6): δ 5.78 (s, 5H, C_5H_5), 1.69 (s, 15H, $C_5(CH_3)_5$), 0.21 (s, 3H, ZrCH_3). ^{13}C NMR (C_6D_6): δ 120.1 (C_5-$(CH_3)_5$), 113.2 (C_5H_5), 34.9 (Zr*C*H$_3$), 11.8 ($C_5(CH_3)_5$). Anal. Calcd $C_{16}H_{23}ClZr$: C, 56.19; H, 6.78. Found: C, 56.15; H, 6.91.

Cp*CpZr(Me)NH^{t}Bu (9). Added to a stirred solution of **8** (0.81 g, 2.4 mmol) in 5 mL of THF was a solution of LiNH^{t}Bu (0.20 g, 2.6 mmol) in 5 mL of THF. The mixture was stirred for 20 h at room temperature, and then the solvent was removed at reduced pressure. The resulting yellow oil was extracted with 10 mL of pentane and filtered through Celite. Removal of pentane at reduced pressure left **9** as an oily yellow solid (0.83 g, 92%). Redissolving this solid in ca. 4 mL of pentane and cooling to −35 °C gave analytically pure **9** as light yellow blocks (0.44 g). ^{1}H NMR (C_6D_6): δ 5.83 (s, 5H, C_5H_5), 4.64 (br s, 1H, NH), 1.73 (s, 15H, $C_5(CH_3)_5$), 1.14 (s, 9H, C(CH_3)$_3$), −0.14 (s, 3H, ZrCH_3). ^{13}C NMR (C_6D_6): δ 115.84 ($C_5(CH_3)_5$), 109.64 (C_5H_5), 56.11 (*C*(CH_3)$_3$), 34.46 (C(*C*H$_3$)$_3$), 20.18 (Zr*C*H$_3$), 11.73 ($C_5(CH_3)_5$). Anal. Calcd $C_{20}H_{33}NZr$: C, 63.43; H, 8.78; N, 3.70. Found: C, 63.08; H, 8.68; N, 3.68.

Cp*Cp(THF)Zr═N^{t}Bu (10a). A solution of **9** (0.94 g, 2.5 mmol) in ca. 10 mL of THF was placed in a glass reaction vessel that was coated with hexamethyldisilazane, heated under a vacuum prior to use, and sealed with a Kontes stopcock. The reaction mixture was then heated at 105 °C for 3 days. The resulting solution was evaporated to leave a yellow solid that was extracted with ca. 5 mL of toluene and filtered. The filtrate was layered with hexanes and cooled to −35 °C, whereupon **10a** crystallized as yellow blocks (2 crops, 0.59 g, 55%). ^{1}H NMR (C_6D_6): δ 6.13 (s, 5H, C_5H_5), 3.45 (m, 4H, OCH_2), 2.02 (s, 15H, $C_5(CH_3)_5$), 1.33 (s, 9H, C(CH_3)$_3$), 1.14 (m, 4H, CH_2). ^{13}C NMR (C_6D_6): δ 116.22 ($C_5(CH_3)_5$), 107.78 (C_5H_5), 77.94 (O*C*H$_2$), 62.25 (*C*(CH_3)$_3$), 35.09 (C(*C*H$_3$)$_3$), 25.64 (*C*H$_2$), 12.46 ($C_5(CH_3)_5$). Anal. Calcd $C_{23}H_{37}NOZr$: C, 63.54; H, 8.58; N, 3.22. Found: C, 63.66; H, 8.83; N, 3.11.

Cp*Cp(THF)Zr═N-*p*-Tol (10b). To a solution of **10a** (107 mg, 0.25 mmol) in 1 mL of toluene was added a solution of **2d** (54 mg, 0.24 mmol) in 2 mL of toluene. A rose color developed immediately. The reaction mixture was left for 3 days at room temperature, and then 3 mL of THF was added. The resulting mixture was transferred to a glass reaction vessel sealed with a Kontes stopcock and heated at 45 °C for 2 days. The solvents were removed at reduced pressure and the resulting brown solid was dissolved in ca. 5 mL of toluene and layered with 10 mL of hexanes. After 4 days at −35 °C, compound **10b** was obtained as orange prisms (77 mg, 67%). ^{1}H NMR (C_6D_6): δ 7.16 (d, 2H, Tol), 6.46 (d, J = 8 Hz, 2H, Tol), 6.03 (s, 5H, C_5H_5), 3.38 (m, 4H, OCH_2), 2.40 (s, 3H, CH_3), 1.92 (s, 15H, $C_5(CH_3)_5$), 1.07 (m, 4H, CH_2). ^{13}C NMR (C_6D_6): δ 160.31 ($C_6H_4CH_3$ (*C*−CH$_3$)), 129.39 (C_6H_4-CH_3 (*o* to CH$_3$)), 121.98 ($C_6H_4CH_3$ (*p* to CH$_3$)), 117.80 ($C_6H_4CH_3$ (*m* to CH$_3$)), 117.29 ($C_5(CH_3)_5$), 108.67 (C_5H_5), 77.86 (O*C*H$_2$), 25.72 (OCH$_2$*C*H$_2$), 21.08 ($C_6H_4CH_3$), 11.89 ($C_5(CH_3)_5$). Repeated attempts to obtain elemental analysis on this complex were not successful. It has been characterized by X-ray diffraction.

Cp*CpZr(N(^{t}Bu)C(Ph)C(Ph)) (11). Diphenylacetylene (29 mg, 0.17 mmol) and **10a** (66 mg, 0.15 mmol) were dissolved in ca. 4 mL of

toluene. A green color developed immediately. After standing for 16 h at room temperature, the reaction mixture was evaporated to dryness and redissolved in ca. 1 mL of toluene. The resulting solution was layered with hexanes and stored at −35 °C. After 3 days, **11** was obtained as green needles (2 crops, 78 mg, 95%). ^{1}H NMR (THF-d_8, 500 MHz): δ 7.50 (d, J = 8 Hz, 1H, Ph), 7.27 (t, J = 8 Hz, 1H, Ph), 7.13 (t, J = 8 Hz, 1H, Ph), 7.05 (t, J = 7 Hz, 1H, Ph), 6.83 (d, J = 8 Hz, 1H, Ph), 6.71 (t, J = 8 Hz, 2H, Ph), 6.49 (t, J = 8 Hz, 1H, Ph), 6.35 (d, J = 8 Hz, 2H, Ph), 6.30 (s, 5H, C_5H_5), 1.91 (s, 15H, $C_5(CH_3)_5$), 1.09 (s, 9H, $C(CH_3)_3$). ^{13}C NMR (THF-d_8, 125 MHz): δ 165.78, 146.52, 138.15, 133.22, 132.24, 131.93, 128.62, 128.17, 127.29, 127.15, 126.36, 120.61 (aromatic, vinylic), 120.14 ($C_5(CH_3)_5$), 111.15 (C_5H_5), 56.82 ($C(CH_3)_3$), 34.92 ($C(CH_3)_3$), 12.12 ($C_5(CH_3)_5$). Anal. Calcd $C_{33}H_{39}NZr$: C, 73.28; H, 7.27; N, 2.59. Found: C, 72.92; H, 7.58; N, 2.51.

$Cp_2Zr(NH$-2,6-$Me_2Ph)(N(Ph)(C(Ph)=CH_2)$(toluene) (13a). $Cp_2Zr(THF)(=N$-2,6-$Me_2Ph)$ (**1b**) (177 mg, 0.429 mmol) and $PhC(Me)=NPh$ (83 mg, 0.429 mmol, 1 equiv) were dissolved in 5 mL of C_6H_6. An orange color developed immediately. After stirring at 25 °C for 1 h, the solvent was removed at reduced pressure to leave an orange solid which was dissolved in toluene (2 mL) and stored at −35 °C. Analytically pure **13a**·toluene was obtained as a yellow powder (180 mg, 82% yield). ^{1}H NMR (C_6D_6): δ 7.71 (m, 2H, aryl), 7.56 (d, J_{H-H} = 7.5 Hz, 2H, aryl), 7.12 (m, 2H, aryl), 7.11 (m, 4H, aryl), 7.06 (m, 3H, aryl), 6.92 (t, J_{H-H} = 7.5 Hz, 1H, aryl), 6.75 (t, J_{H-H} = 7 Hz, 1H, aryl), 6.44 (s, 1H, N*H*, 5.70 (s, 10H, C_5H_5), 5.48 (s, 1H, vinyl C*H*), 4.50 (s, 1H, Vinyl C*H*), 1.85 (s, 6H, CH_3), 1.83 (s, 3H, CH_3) ppm. ^{13}C NMR (C_6D_6): δ 158.95, 156.61, 156.01, 140.80, 129.28, 128.65, 128.51, 128.43, 128.29, 127.86, 127.81, 127.51, 125.64, 122.44, 122.02, 118.55, 111.88, 107.49, 21.37, 20.68 ppm. Anal. Calcd $C_{39}H_{40}N_2Zr$: C, 74.59; H, 6.42; N, 4.46. Found: C, 74.34; H, 6.56; N, 4.59.

Cp*CpZr(NH^{t}Bu)(N(Ph)C(Ph)=CH$_2$) (13b). A solution of ketimine **2l** (43 mg, 0.22 mmol) in ca. 5 mL of toluene was added to a solution of **10a** (96 mg, 0.22 mmol) in ca. 5 mL of toluene. The solution slowly developed an orange color. After 1 day, the solvent was evaporated at reduced pressure, and the resulting red-brown oil was dissolved in hexanes, filtered and stored at −35 °C. After 6 months, **13b**·0.5hexane was obtained as orange plates (80 mg, 61%). ^{1}H NMR (C_6D_6): δ 7.65 (d, J = 8 Hz, 2H, Ph), 7.10 (m, 6H, Ph), 6.97 (t, J = 8 Hz, 1H, Ph), 6.68 (t, J = 8 Hz, 1H, Ph), 6.10 (s, 5H, C_5H_5), 5.63 (br s, 1H, CH_2), 5.36 (br s, 1H, CH_2), 4.6 (v br, 1H, N*H*), 1.76 (s, 15H, $C_5(CH_3)_5$), 1.22 (br s, 9H, $C(CH_3)_3$). ^{13}C NMR (C_6D_6, 125 MHz, 60 °C): δ 160.59, 155.70, 141.73, 128.36, 127.92, 127.65, 127.21, 123.37 (br), 117.22 (br), 107.92 (br) (aromatic, vinylic), 120.07 ($C_5(CH_3)_5$), 111.95 (C_5H_5), 59.13 ($C(CH_3)_3$), 34.06 ($C(CH_3)_3$), 12.84 ($C_5(CH_3)_5$). Anal. Calcd $C_{33}H_{42}N_2Zr$: C, 71.04; H, 7.59; N, 5.02. Found: C, 71.12; H, 7.34; N, 5.06.

X-ray Structure Determination of 3d, 10a, 10b, and 13b. All crystals were mounted on quartz fibers using Paratone N hydrocarbon oil. For all compounds, measurements were made on a SMART CCD area detector with graphite monochromated Mo−Kα radiation. Data were integrated by the program SAINT. The data were corrected for Lorentz and polarization effect, and analyzed for agreement and possible absorption using XPREP.[33] An empirical absorption correction was made based on comparison of redundant and equivalent reflections as applied using SADABS[34] (**3d**, T_{max} = 0.96, T_{min} = 0.70; **10a**, T_{max} = 0.897, T_{min} = 0.818; **10b**, T_{max} = 0.97, T_{min} = 0.81). The structures were solved by direct methods and expanded using Fourier techniques. The non-hydrogen atoms were refined anisotropically. Plots of $\sum w(|F_o| - |F_c|)^2$ versus $|F_o|$, reflection order in data collection, $(\sin\theta)/\lambda$, and various classes of indices showed no unusual trends. All calculations were performed using the teXsan[35] crystallographic software package of Molecular Structure Corp.

Table 5. Crystallographic Data for Compounds **3d**, **10a**, **10b**, and **13b**

	3d	**10a**	**10b**	**13b**·0.5 C_6H_{14}
formula	$C_{38}H_{38}N_2Zr$	$C_{23}H_{37}NOZr$	$C_{26}H_{35}NOZr$	$C_{33}H_{42}N_2Zr$
fw	613.95	434.77	468.79	557.94
color	blue, plate	yellow, block	orange, plate	yellow, plate
cryst syst	monoclinic	orthorhombic	monoclinic	monoclinic
lattice type	primitive	primitive	primitive	primitive
temp (K)	168	168	168	168
space group	$P2_1/n$ (#14)	$Pbcn$ (#60)	$P2_1/c$ (#14)	$P2_1/n$ (#14)
a, Å	11.2145(7)	28.7306(3)	8.8942(3)	8.8470(1)
b, Å	13.5719(9)	10.3514(1)	17.2473(6)	20.9552(1)
c, Å	20.1565(13)	15.1662(1)	15.8147(5)	16.9649(2)
α, deg	90.00	90.00	90.00	90.00
β, deg	95.345(1)	120.00	105.3750(10)	94.767(1)
γ, deg	90.00	90.00	90.00	90.00
V, Å^3	3054.5(3)	4510.46(6)	2339.17(12)	4510.46(6)
Z	4	8	4	4
μ(MoKα) cm^{-1}	3.89	4.98	4.86	4.29
D_{calc}, g/cm^3	1.335	1.28	1.331	1.339
total data	13796	21627	11027	14671
residuals: R; R_w	0.040; 0.040	0.028; 0.032	0.033; 0.035	0.036; 0.039
GOF	1.21	1.44	1.38	1.47
radiation	Mo Kα (λ = 0.710 69 Å) graphite monochromated			

Crystallographic data for compounds **3d**, **10a**, **10b**, and **13b** are listed in Table 5, and selected bond lengths and bond angles are given in Table 3; full details are given in the Supporting Information.

Kinetic Studies. In a typical experiment, a stock solution of **6b** (134.7 mg, 0.267 mmol) and diphenylacetylene (47.6 mg, 0.267 mmol) in 2.00 mL C_6D_6 was prepared in a volumetric flask. The imines $PhCH=N$-*p*-Tol and *p*-F-$C_6H_4CH=N$-*p*-F-C_6H_4 were weighed into a vial and a 1-mL volumetric flask, respectively. The stock solution of **6b** and diphenylacetylene (150 μL) was added to the 1-mL volumetric flask. The imine $PhCH=N$-*p*-Tol was dissolved in C_6D_6 and transferred to the 1-mL volumetric flask, rinsing twice. The volumetric flask was diluted to the final volume, the solution was mixed well, and 0.5 mL of the solution was transferred to a NMR tube. The tube was attached to a cajon adapter and was flame-sealed under vacuum. The tube was heated in a 105 °C constant temperature silicone oil bath. Heating times were monitored with a stopwatch. At selected time intervals, the tube was immersed in an ice water bath (the metathesis reaction was not observed at ambient temperature or below). Eight data points were obtained by ^{1}H NMR spectroscopy over 907 min reaction time.

Acknowledgment. We thank Drs. Frederick Hollander and Ryan Powers for solving the crystal structures of **3d**, **10a**, **10b**, and **13b**, the National Institutes of Health (Grant no. GM-25459) for financial support of this work, and Prof. Tara Y. Meyer (University of Pittsburgh) for her willingness to exchange data prior to publication.

Supporting Information Available: Crystallographic data for **3d**, **10a**, **10b**, and **13b** and kinetic plots for the rate and simulation study. This material is available free of charge via the Internet at http://pubs.acs.org.

JA992869R

(33) XPREP, v. 5.03 (part of the SHELXTL Crystal Structure Determination Package); Siemens Industrial Automation, Inc., 1995.

(34) Sheldrick, G. SADABS: Siemens Area Detector Absorption correction program; Siemens Industrial Automation, Inc., 1996.

(35) teXsan: Crystal Structure Analysis Package; Molecular Structure Corp., 1985 and 1992.